



## Stick-Slip Vibrations Induced by Alternate Friction Models

R. I. LEINE, D. H. VAN CAMPEN, and A. DE KRAKER

*Department of Mechanical Engineering, Eindhoven University of Technology, P.O. Box 513,  
5600 MB Eindhoven, The Netherlands*

L. VAN DEN STEEN

*Shell International Exploration and Production B.V., P.O. Box 60, 2280 AB Rijswijk, The Netherlands*

(Received: 12 June 1997; accepted: 8 January 1998)

**Abstract.** In the present paper a simple and efficient alternate friction model is presented to simulate stick-slip vibrations. The alternate friction model consists of a set of ordinary non-stiff differential equations and has the advantage that the system can be integrated with any standard ODE-solver. Comparison with a smoothing method reveals that the alternate friction model is more efficient from a computational point of view. A shooting method for calculating limit cycles, based on the alternate friction model, is presented. Time-dependent static friction is studied as well as application in a system with 2-DOF.

**Keywords:** Stick-slip vibrations, shooting method, dry friction, discontinuous systems.

### 1. Introduction

The presence of friction-induced self-sustained vibrations can be highly detrimental to the performance of mechanical systems. Two general forms of friction-induced vibration may be identified, namely, stick-slip and quasi-harmonic oscillation [6, 10]. Stick-slip vibration is characterized by a sawtooth displacement-time evolution which has clearly defined stick and slip phases in which the two surfaces in contact stick respectively slip over each other. The motion is governed by a static friction force in the stick phase and a velocity dependent kinetic friction force in the slip phase. On the other hand, quasi-harmonic friction-induced vibration has a nearly sinusoidal displacement-time evolution and the motion is initiated and maintained in the slip phase. Quasi-harmonic friction-induced vibration is caused by a hump in the friction-velocity profile [6].

The first step to reduce or avoid these vibrations is to create a representative numerical model that can be used to evaluate all possible phenomena and can be incorporated in a control system. The study of stick-slip vibrations is faced with difficulties, as during the stick-slip motion two different mechanisms take place. The modeling of the static friction mechanism and that of the kinetic friction mechanism yield a set of differential equations with discontinuous right-hand side.

A standard method to solve discontinuous differential equations consists of applying a smoothing method (also called normalization method). The smoothing method [13, 18, 19, 23] replaces the discontinuous system by a smooth adjoint system. The smoothing method yields a system of ordinary but stiff differential equations and consequently leads to large computational times.

The problems of the smoothing method led to the development of models which switch between different sets of equations, the so-called ‘alternate friction models’ or ‘switch models’. Many researchers studied stick-slip vibrations with switch models similar to the switch model of Pfeiffer [14, 18, 21]. The switch model of [17] starts from an initial state with a set of differential equations. After each timestep the state vector is inspected on a possible event within this timestep (e.g. slip to stick transition). If an event happened, the integration process is halted and an iteration procedure is started to find the switching point (within a certain range of accuracy). Having thus evaluated the switching point, a new integration process is started with a modified set of differential equations and initial conditions identical to the state at the switching point.

The need to halt the integration process, determine the discontinuity with an iteration process and restart the integration again is undesirable from a numerical point of view. Standard integration methods integrate a set of differential equations over a specified time interval. So, if the integration needs to be halted at the discontinuity, standard integration methods cannot be applied.

In the present paper a simple and efficient switch model is presented to simulate stick-slip vibrations. The specific switch model presented here consists of a set of ordinary non-stiff differential equations. This has the advantage that the system can be integrated with any standard ODE-solver available in mathematical packages (MATLAB, MATHEMATICA, MAPLE) or ODE-solvers of existing software libraries (NAG). The system is thus integrated without the need to halt which minimizes start-up costs.

The shooting method as a periodic solution finder in combination with a smoothing method, was applied in [23] to find periodic stick-slip solutions. Shooting methods as periodic solution solvers in combination with switch models have not been addressed in the past. The current paper presents a method to combine shooting with the proposed switch model. A brief introduction on the standard shooting method will be given first.

## 2. Shooting Method

A number of algorithms are available for finding periodic solutions. The shooting method is probably the most popular one [4, 16, 22], and will be discussed in this section.

Consider an  $n$ th-order, autonomous, nonlinear dynamic system represented by the state equation

$$\dot{\underline{x}} = \underline{f}(\underline{x}), \quad (1)$$

where  $\dot{\underline{x}} \equiv d\underline{x}/dt$ ,  $\underline{x}$  is a column with the  $n$  state variables of the system,  $t$  is time and  $\underline{f}$  is a column of nonlinear functions of the components of  $\underline{x}$ . Since  $\underline{f}$  does not depend on  $t$ , the system is called autonomous, as opposed to non-autonomous systems, where  $\underline{f}$  is a function of both  $\underline{x}$  and  $t$ . In the following, only autonomous systems are dealt with.

In an initial-value problem, the initial condition is usually given at  $t = t_0$ . Because  $\underline{f}$  is independent of  $t$ , solutions based at time  $t_0 \neq 0$ , can always be translated to  $t_0 = 0$ . Hence, the initial condition reads

$$\underline{x}(t = 0) = \underline{x}_0. \quad (2)$$

The solution to Equation (1), satisfying (2) is often written as  $\phi_t(\underline{x}_0)$ , to explicitly show the dependence on the initial condition in (2).

The shooting method finds periodic solutions of the system by solving a two-point boundary-value problem, in which solutions are sought of

$$\underline{H}(\underline{x}_0, T) \equiv \underline{\phi}_T(\underline{x}_0) - \underline{x}_0 = \underline{0}, \quad (3)$$

where  $T$  is the period time of the periodic solution and  $\underline{x}_0$  is a state on the limit cycle. Since Equation (3) is a system of  $n$  equations in  $n+1$  unknowns (the  $n$  components of  $\underline{x}_0$  and period  $T$ ), it cannot be solved directly. Instead,  $\underline{y} \equiv \underline{H}(\underline{x}_0, T)$  is linearized, to obtain

$$\Delta \underline{y} \approx \frac{\partial \underline{H}}{\partial \underline{x}_0} \Delta \underline{x}_0 + \frac{\partial \underline{H}}{\partial T} \Delta T = (\underline{\Phi}_T(\underline{x}_0) - \underline{I}) \Delta \underline{x}_0 + \underline{f}(\underline{\phi}_T(\underline{x}_0)) \Delta T, \quad (4)$$

where the matrix  $\underline{\Phi}_T(\underline{x}_0)$  results from the variational equation (see Appendix A). To achieve  $\underline{H} \approx \underline{0}$ ,  $\Delta \underline{x}_0$  and  $\Delta T$  will be chosen in such a way that  $\Delta \underline{y} = -\underline{H}$ . This value of  $\Delta \underline{y}$  is inserted into Equation (4), giving

$$-\underline{H} = (\underline{\Phi}_T(\underline{x}_0) - \underline{I}) \Delta \underline{x}_0 + \underline{f}(\underline{\phi}_T(\underline{x}_0)) \Delta T. \quad (5)$$

To make this system solvable, a constraint is added, which restricts the state correction term  $\Delta \underline{x}_0$  to be orthogonal to  $\underline{f}$ , given by

$$\underline{f}(\underline{x}_0)^T \Delta \underline{x}_0 = 0. \quad (6)$$

From Equations (5) and (6), the following iterative scheme is assembled, with which zeros of  $\underline{H}$  can be found, using initial guesses  $\underline{x}_0^{(0)}$  and  $T^{(0)}$

$$\begin{bmatrix} \underline{\Phi}_{T^{(i)}}(\underline{x}_0^{(i)}) - \underline{I} & \underline{f}(\underline{\phi}_{T^{(i)}}(\underline{x}_0^{(i)})) \\ \underline{f}(\underline{x}_0^{(i)})^T & 0 \end{bmatrix} \begin{bmatrix} \Delta \underline{x}_0^{(i)} \\ \Delta T^{(i)} \end{bmatrix} = \begin{bmatrix} \underline{x}_0^{(i)} - \underline{\phi}_{T^{(i)}}(\underline{x}_0^{(i)}) \\ 0 \end{bmatrix}, \quad (7)$$

$$\begin{bmatrix} \underline{x}_0^{(i+1)} \\ T^{(i+1)} \end{bmatrix} = \begin{bmatrix} \underline{x}_0^{(i)} \\ T^{(i)} \end{bmatrix} + \begin{bmatrix} \Delta \underline{x}_0^{(i)} \\ \Delta T^{(i)} \end{bmatrix}. \quad (8)$$

The superscripts have been added to indicate the iteration count. This scheme is reiterated, until some convergence criterion is met. There is a clear similarity to the Newton–Raphson algorithm, so the same convergence properties apply. When the shooting method returns values  $\underline{x}_0$  and  $T$ , it should be tested, whether  $T$  is the minimum period of the solution, since it could be a multiple of the actual period. Only single shooting is considered in this paper for reasons of simplicity.

### 3. Single-Degree-of-Freedom Model

A single-degree-of-freedom model will be used to introduce and evaluate the numerical methods described in this paper. The same model treated in [7, 23] is used to facilitate the comparison of results. Consider a mass  $m$  attached to inertial space by a spring  $k$ , where  $m = 1$  [kg] and  $k = 1$  [N/m]. The mass is riding on a driving belt, that is moving at constant velocity  $v_{\text{dr}} = 0.2$  [m/s] (Figure 1).

Between mass and belt, dry friction occurs, with a friction force  $F$ . The state equation, describing this model, reads

$$\dot{\underline{x}} = \underline{f}(\underline{x}) = \begin{bmatrix} \dot{x} \\ -\frac{k}{m}x + \frac{F}{m} \end{bmatrix}, \quad (9)$$

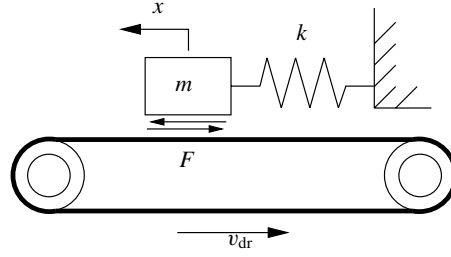


Figure 1. 1-DOF model with dry friction.

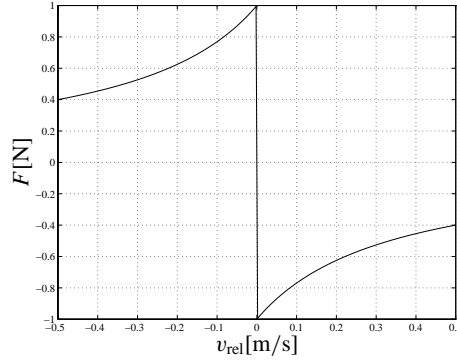


Figure 2. Friction as a function of relative velocity.

where a dot ( $\dot{\cdot}$ ) denotes differentiation with respect to time  $t$  and  $\underline{x} = [x \ \dot{x}]^T$ . The relative velocity of the mass  $m$  with respect to the belt is denoted by  $v_{\text{rel}} = \dot{x} - v_{\text{dr}}$ . The friction force  $F$  is in the slip phase a function of the relative velocity  $v_{\text{rel}}$  and in the stick phase a function of the externally applied force. The externally applied force on the mass is in this case the force in the spring and is thus only dependent on the displacement:

$$F_{\text{ex}}(x) = kx. \quad (10)$$

The friction model reads

$$F(v_{\text{rel}}, x) = \begin{cases} F(x) = \min(|F_{\text{ex}}(x)|, F_s) \operatorname{sgn} F_{\text{ex}}(x), & v_{\text{rel}} = 0 \text{ stick,} \\ F(v_{\text{rel}}) = -\frac{F_s \operatorname{sgn} v_{\text{rel}}}{1 + \delta|v_{\text{rel}}|}, & v_{\text{rel}} \neq 0 \text{ slip.} \end{cases} \quad (11)$$

The friction force in the stick phase is limited by the maximum static friction force, i.e.  $|F(x)| \leq F_s$ , and  $F_s$  is chosen equal to 1 [N]. The friction curve is drawn in Figure 2. The constant  $\delta$  is taken to be 3 [s/m].

#### 4. Smoothing Method

For the classical application of the shooting method it is necessary that the fundamental solution matrix is a continuous function in time. This implies that the state equation function  $f$  must be continuous. However, the system (9) together with the friction model (11) is

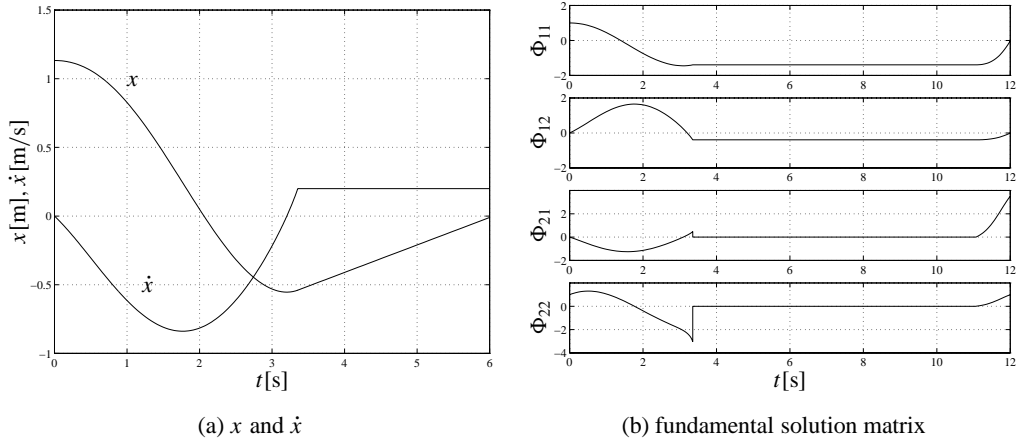


Figure 3. Results obtained with the approximated friction curve ( $\varepsilon = 10^6$ ).

discontinuous. The friction curve is therefore often approximated by a smooth function. One possible approximation for  $F$  is [23]

$$\tilde{F}(v_{\text{rel}}) = -\frac{F_s \frac{2}{\pi} \arctan \varepsilon v_{\text{rel}}}{1 + \delta |v_{\text{rel}}|}. \quad (12)$$

Clearly, increasing the steepness parameter  $\varepsilon$  improves the approximation, especially for  $v_{\text{rel}}$  close to 0. The friction curve will almost be the same as in Figure 2 for large values of the steepness parameter ( $\varepsilon = 10^6$ ). However, a steep slope in  $\tilde{F}$  arises at  $v_{\text{rel}} = 0$ , given by  $-(2/\pi)\varepsilon F_s$ . This causes a stiff differential equation, which is numerically costly to integrate.

The evolution in time of the displacement  $x$  and the velocity  $\dot{x}$  is shown in Figure 3a for  $\varepsilon = 10^6$ . More interesting is the evolution of the elements of the fundamental solution matrix (Figure 3b). Near the transition from the slip phase to the stick phase the fundamental solution varies extremely fast. The time derivatives of these functions become unbounded as  $\varepsilon$  approaches infinity. The fundamental solution matrix elements associated with the unapproximated friction curve exhibit a jump at this point.

Where the solution  $\underline{x}$  is still continuous, the fundamental solution matrix clearly is not, which makes it difficult to integrate for large values of  $\varepsilon$ . The approximated friction curve can be seen as a singular perturbation [4]. If we let  $\varepsilon$  approach infinity, the order of the system reduces and the perturbation becomes singular. The class of boundary-value problems involving singular perturbations has been a source of difficulty up to now.

## 5. The Switch Model

Another method of integrating the system of equations is by using the Karnopp friction model [3, 8, 11]. The classical Karnopp model has the advantage of generating ordinary differential equations but suffers from some numerical instabilities in the stick phase [20]. The switch model as proposed in this paper, does not possess this disadvantage and can be considered to be an improved version of the Karnopp model. It treats the system as three different sets of ordinary differential equations: one for the slip phase, a second for the stick phase and a third for the transition from stick to slip. At each timestep the state vector is inspected to determine

whether the system is in the slip mode, in the stick mode or in the transition mode. The corresponding time derivative of the state vector is then chosen. The conditions for changing to the stick mode or the slip mode operate as switches between the systems. A region of small velocity is defined as  $|v_{\text{rel}}| < \eta$ , where  $\eta \ll v_{\text{dr}}$ . The system is considered to be in the slip mode if the relative velocity lies outside this narrow stick band. The finite region is necessary for digital computation since an exact value of zero will rarely be computed. If the relative velocity lies within the stick band and if the static friction force, needed to make equilibrium with the applied forces on the mass, exceeds the breakaway friction force  $F_s$ , the system is considered to be in transition from stick to slip. The switch model can be elucidated in pseudo code:

```

if  $|v_{\text{rel}}| > \eta$  then
     $\dot{\underline{x}} = \underline{f}(\underline{x}) = \begin{bmatrix} \dot{x} \\ -\frac{k}{m}x + \frac{F(v_{\text{rel}})}{m} \end{bmatrix}$     slip
elseif  $|kx| > F_s$ 
     $\dot{\underline{x}} = \underline{f}(\underline{x}) = \begin{bmatrix} \dot{x} \\ -\frac{k}{m}x + \frac{F_s}{m} \text{sgn } kx \end{bmatrix}$     stick to slip transition
else
     $\dot{\underline{x}} = \underline{f}(\underline{x}) = \begin{bmatrix} v_{\text{dr}} \\ -v_{\text{rel}}\sqrt{\frac{k}{m}} \end{bmatrix}$     stick
end;

```

The collocation points of the Runge–Kutta integration method during the stick mode should all be situated within the stick band to avoid numerical instability problems of the Karnopp model. This can be achieved by centering the relative velocity in the stick band and taking a Runge–Kutta tolerance smaller than  $\eta$ . The acceleration of the mass during the stick mode is set to  $-v_{\text{rel}}\sqrt{k/m}$  to force the relative velocity to zero. The relative velocity, which is directly dependent on the state of the system, cannot simply be set to zero in the stick phase as the state vector has to be continuous for ordinary differential equations. The proposed algorithm maintains the continuity of the state vector and yields a set of ordinary differential equations without numerical instabilities.

The fundamental solution matrix is not Lipschitz continuous as it jumps at the transition from stick to slip. The monodromy matrix for the switch model cannot be obtained in the same way as in the previous section. Instead, the monodromy matrix is determined by applying a sensitivity analysis to the solution using the relation

$$\delta \underline{x}(t) = \underline{\Phi}_t(\underline{x}_0) \delta \underline{x}_0. \quad (13)$$

We perturb one component (say component  $j$ ) of the initial state vector with a small perturbation and leave the other components unaltered

$$\tilde{\underline{x}}_0^j = \underline{x}_0 + \delta \underline{x}_0^j, \quad (14)$$

with

$$\delta \underline{x}_0^j = \begin{bmatrix} 1 & \dots & 0 & \xi^j & 0 & \dots & 0 \end{bmatrix}^T, \quad (15)$$

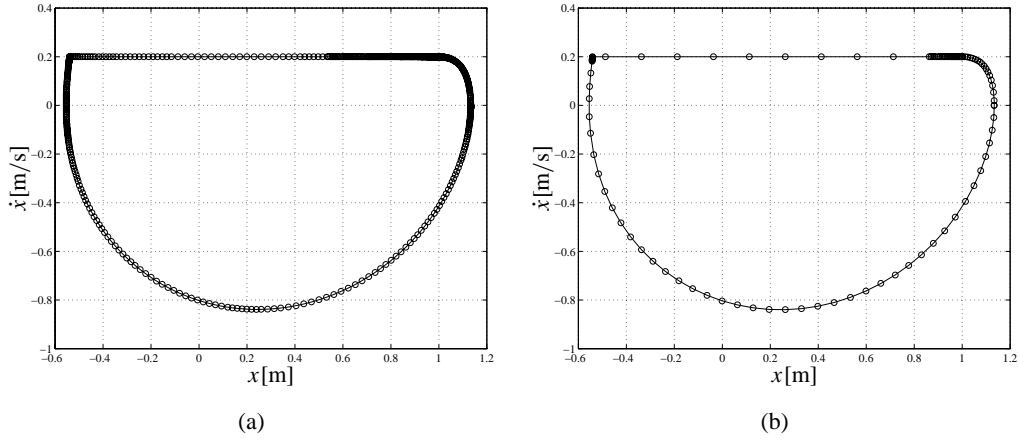


Figure 4. Phase portraits obtained with the smoothing method ( $\varepsilon = 10^6$ ) (a) and with the switch model (b).

where  $\xi \ll x_{0_j}$ . In the above,  $x_{0_j}$  denotes the  $j$ -th element of  $\underline{x}_0$  while a superscript  $j$  indicates which element in the initial state vector is perturbed. The system can be integrated over the period time  $T$  with  $\tilde{\underline{x}}_0^j$  as initial state vector yielding  $\tilde{\underline{x}}_T^j$ . The perturbation of the initial state vector causes a perturbation of the final state vector

$$\delta \underline{x}_T^j = \tilde{\underline{x}}_T^j - \underline{x}_T. \quad (16)$$

The elements of the monodromy matrix can then be expressed as

$$\Phi_{T_{ij}} = \frac{\delta x_{T_i}^j}{\xi}. \quad (17)$$

The shooting method can now be applied to the switch model using the monodromy matrix obtained by the above sensitivity analysis giving an altered (single) shooting method.

A phase portrait obtained with the switch model for the single-DOF system of Section 3 is depicted in Figure 4b. The computation took 110232 floating-point-operations to obtain a shooting accuracy of  $10^{-5}$  with a Runge–Kutta–Fehlberg tolerance of  $10^{-8}$ . Small timesteps are taken only near the transitions between slip and stick phase, resulting in 123 integration points in the final limit cycle. In fact, the adaptive timestep control of the integration algorithm determines the switching point with the desired accuracy. The constant  $\eta$  was taken to be  $10^{-6}$ . The initial guess for the state vector was  $\underline{x}_0 = [1.1, 0]^T$ , whereas for the period time it was  $T_0 = 12$ . In Figure 4a the results obtained with the smoothing method are plotted for  $\varepsilon = 10^6$ . A Backward Differentiation Formula (BDF) proved to be the best integration method for the extremely stiff differential equation. This computation took 3493510 floating-point-operations to obtain the same accuracy as in the previous case starting from the same initial guess. Small timesteps are not only necessary near the transitions but during the whole stick phase, resulting in 1217 integration points. The smoothing method needed 31.7 times more floating point operations and about 10 times more data storage. Consequently, the smoothing method is clearly more expensive than the switch model.

While using the smoothing method, the friction force should be a continuous function of velocity. If an isolated static friction point was added to the discontinuous friction curve, a

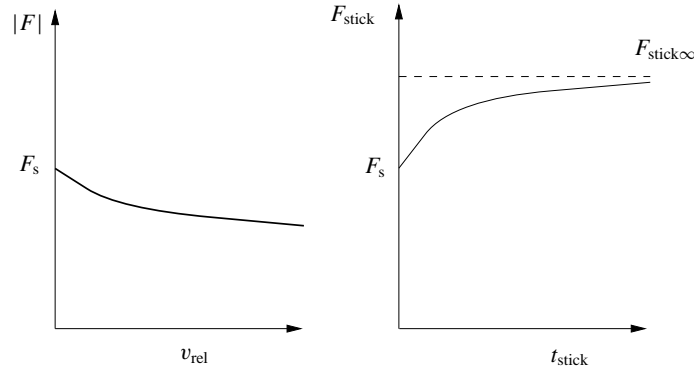


Figure 5. Time-dependent static friction model.

second steep slope would be added to the smooth approximation yielding an even more stiff differential equation. The switch model can easily be extended with an isolated static friction point. The small timesteps just after stick to slip transition in Figure 4a are due to a continuous transition from a static to a dynamic friction force. The addition of an isolated static friction point would limit this region of refinement and speed up the integration process.

## 6. Time-Dependent Static Friction

An important advantage of the switch model is the possibility of incorporating tribological enhancements of the classical friction model treated in the previous section. One of the main phenomena not captured by the classical friction model is time-dependent static friction [2, 3, 9]. Although time-dependent static friction may not be significant in ‘stiff’ constructions it can play a roll in low-frequency dynamical systems with a pronounced stick time. During sticking, the friction force rises until a maximum is reached: the static friction force (also known as breakaway friction force). The time-dependent static friction model considers the static friction force to be dependent on the stick time. The static friction force is depicted in Figure 5 and can be expressed as [12]

$$F_{\text{stick}} = F_s(1 + (\beta - 1)(1 - e^{-at_{\text{stick}}}), \quad (18)$$

where  $\beta = F_{\text{stick}\infty}/F_s$ . The dependence of the dynamic friction force on the relative velocity is drawn in the left part of Figure 5 and is considered to be symmetrical.

If we try to incorporate the time-dependent static friction force in the switch model, we are faced with a difficulty inherent to the physical problem. The stick time has to be known during sticking. The most straightforward solution is to consider the stick time as an extra state of the system, thus preserving the set of differential equations to be ordinary. The state vector is extended with the stick time state  $\mathbf{x} = [x \ \dot{x} \ t_{\text{stick}}]^T$ . The stick time state has to be zero at the beginning of the stick phase. Consequently, the stick time state has to decrease during the slip phase to zero. It does not matter how it decreases, as long as the final value of the stick time state is approximately zero. However, stiff differential equations will arise if the slope is taken very large. The decrease will be modeled with an exponentially decaying function  $e^{-bt}$ . The extended pseudo code for the time-dependent static friction model is:

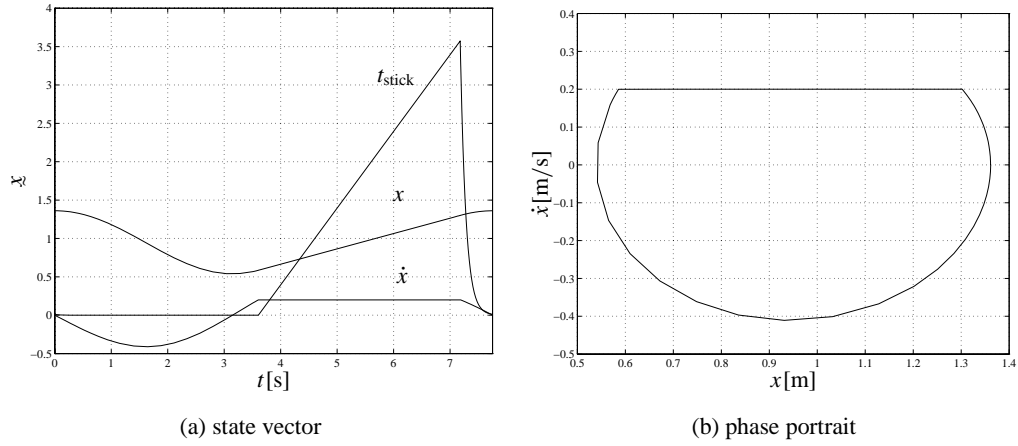


Figure 6. Periodic solution of the time-dependent static friction model.

**if**  $|v_{rel}| > \eta$  **then**

$$\dot{x} = \underline{f}(x) = \begin{bmatrix} \dot{x} \\ -\frac{k}{m}x + \frac{F(v_{rel})}{m} \\ -bt_{stick} \end{bmatrix} \quad \text{slip}$$

**elseif**  $|kx| > F_{stick}$

$$\dot{x} = \underline{f}(x) = \begin{bmatrix} \dot{x} \\ -\frac{k}{m}x + \frac{F_{stick}}{m} \operatorname{sgn} kx \\ -bt_{stick} \end{bmatrix} \quad \text{stick to slip transition}$$

**else**

$$\dot{x} = \underline{f}(x) = \begin{bmatrix} v_{dr} \\ -v_{rel}\sqrt{\frac{k}{m}} \\ 1 \end{bmatrix} \quad \text{stick}$$

**end;**

A periodic solution of the time-dependent static friction model obtained with the shooting method is drawn in Figure 6 ( $a = 0.1$  [1/s],  $b = 10$  [1/s],  $\beta = 2$ ). The phase portrait is not only shifted to the right, due to a higher static friction force, but also shows a non-smooth transition from stick to slip phase due to a difference between static and dynamic friction force.

## 7. Example: A Violin String

The switch model can also be used for systems with greater complexities. Consider a single violin string with radius  $r$  and a bow that is moving at a constant velocity  $v_{dr}$  over the string (Figure 7). The friction force between bow and string will induce the lateral displacement  $x$

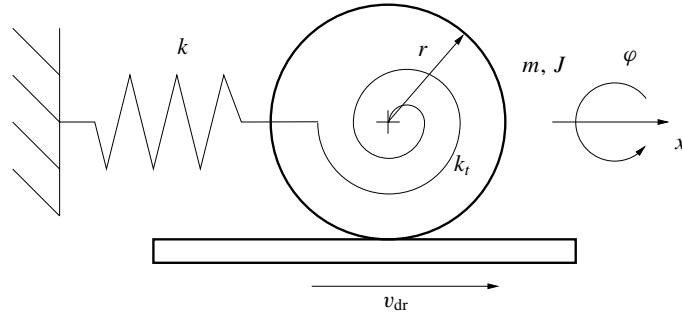


Figure 7. Simple model of a violin string.

and rotation  $\varphi$  (2-DOF). With the state vector  $\underline{x} = [x \ \dot{x} \ \varphi r \ \dot{\varphi} r]^T$  the equations of motion in the slip phase yield:

$$\dot{\underline{x}} = \begin{bmatrix} \dot{x} \\ -\frac{k}{m}x + \frac{F(v_{\text{rel}}, x, \varphi)}{m} \\ \dot{\varphi} r \\ -\frac{k_t}{J}\varphi r + \frac{F(v_{\text{rel}}, x, \varphi)r^2}{J} \end{bmatrix}. \quad (19)$$

The friction force is defined by Equations (11) and (10) is replaced by the externally applied force on the interface,

$$F_{\text{ex}}(x, \varphi) = \frac{kx + k_t \frac{m}{J} \varphi r}{1 + r^2 \frac{m}{J}}. \quad (20)$$

The relative velocity is dependent on the lateral vibration as well as on the torsional vibration,

$$v_{\text{rel}} = \dot{x} + \dot{\varphi} r - v_{\text{dr}}. \quad (21)$$

Figure 8a displays the phase portrait for the lateral vibration. The starting solution for the shooting method is created by a simple time integration process. More or less representative parameter values can be found in Appendix B. In the stick phase, the string rolls over the bow with an angular velocity of  $\dot{\varphi} = (\dot{x} - v_{\text{dr}})/r$ . The lateral velocity is therefore not constant in the stick phase. The periodic solution of the corresponding 1-DOF (block-on-belt) model is drawn with a dashed line in the same plot. It approximates the 2-DOF violin string model very well.

If the diameter of the string is reduced to  $d = 0.25$  mm, the qualitative behaviour changes drastically (Figures 8b and 9b). Again, the 1-DOF solution is plotted with a dashed line (Figure 8b). It differs significantly from the 2-DOF solution. No periodic solution was found for this case. The obtained solution is possibly chaotic or quasi-periodic. As shown in Figure 10, the frequency spectrum for the second case is quite different from the periodic solution of the first case. It has a broad-band nature.

The frequency ratio of the torsional vibrations relative to the lateral vibrations is proportional to the diameter.

$$\frac{\omega_t}{\omega_l} = \frac{\sqrt{k_t/J}}{\sqrt{k/m}} = \sqrt{\frac{GA}{f_t}} = \frac{d}{2} \sqrt{\frac{\pi G}{f_t}}.$$

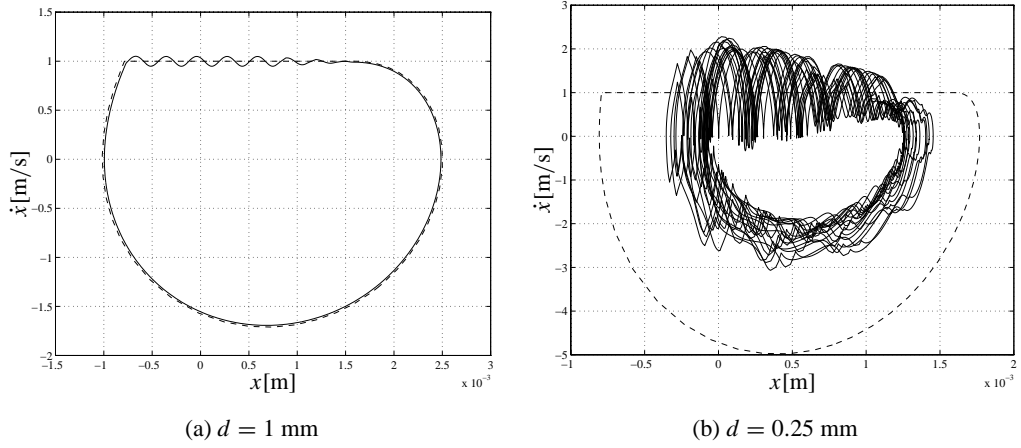


Figure 8. Phase portraits of the violin string model.

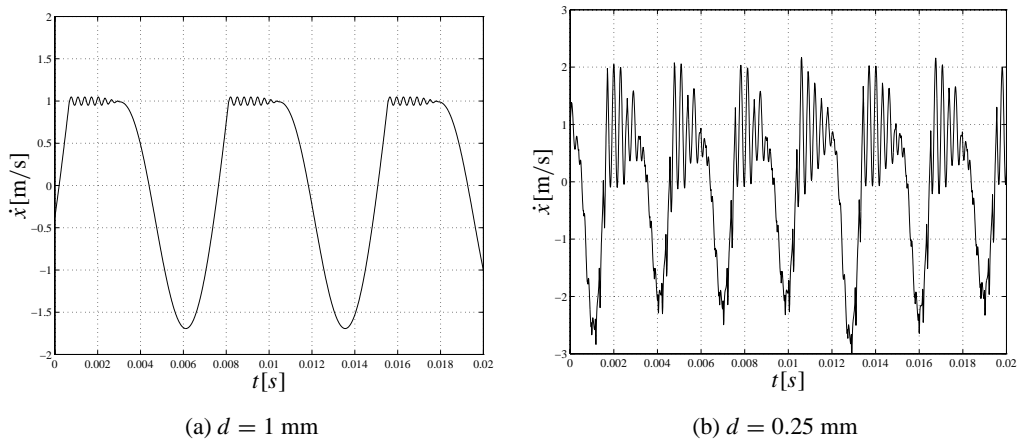


Figure 9. Time histories.

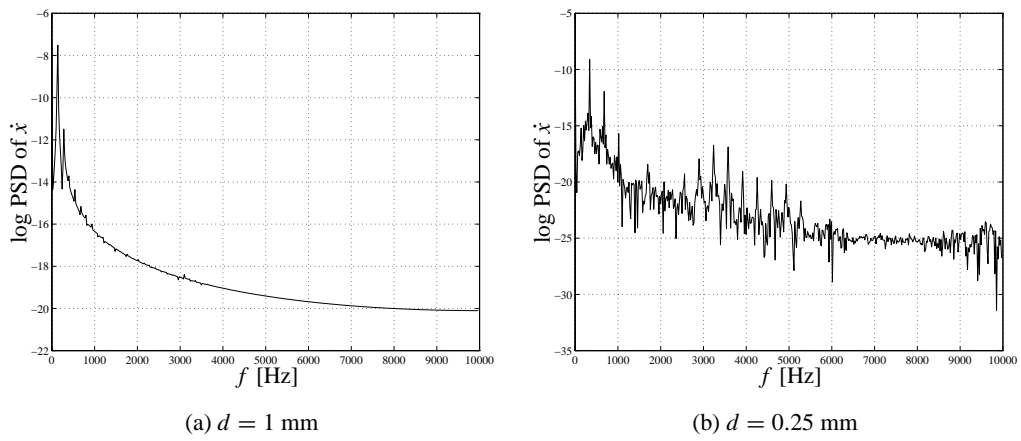


Figure 10. Power spectral density plots.

The torsional vibrations did not have significant influence for  $d = 1$  mm because the torsional frequency was much higher than the lateral frequency ( $\omega_t/\omega_1 = 35.3$ ). Decreasing the diameter of the string to  $d = 0.25$  mm reduced the frequency ratio ( $\omega_t/\omega_1 = 8.8$ ) and increased the effect of the torsional mode.

## 8. Conclusions

Finding periodic solutions of stick-slip vibrations using the smoothing method is very expensive, even for a simple 1-DOF problem. In the present paper a simple and efficient switch model was presented to simulate stick-slip vibrations. The switch model consists of a set of ordinary non-stiff differential equations and has the advantage that the system can be integrated with any standard ODE-solver. The system is thus integrated without the need to halt, which minimizes start-up costs. It is shown that a smooth friction curve is not essential for the application of the shooting method as periodic solution finder. A method to combine shooting with the proposed switch model was presented. If the friction curve described by Equation (11) is the best representation of reality, then the switch model yields the best results. On the other hand, one could argue whether the real friction curve would look more like the approximated friction curve where the slip during the stick phase can be regarded as micro-slip. In this case, the switch model is still a good and efficient approach due to the fact that the steepness parameter  $\varepsilon$  is extremely large in practice. The approximated friction curve can only model the plastic part of the micro-slip and not the elastic part. A full description of micro-slip would again point to the direction of a switch model. It has been shown that the switch model can be extended with tribological enhancements to the classical friction model. The application of the switch model in a 2-DOF system has been presented.

## 9. Further Research

The application of the switch model to systems with many degrees-of-freedom as well as the use in control systems will be studied in future research.

In [1, 5, 15] the method of Aizerman and Gantmakher is described to determine the fundamental solution matrix of discontinuous systems in order to calculate Lyapunov exponents. The theory of Aizerman and Gantmakher could also be used in a shooting method and this will also be an aim in further research.

## Acknowledgments

This project was supported by the Dutch Technology Foundation, STW. The authors are much indebted to the anonymous reviewers for useful comments.

## Appendix A: The Variational Equation

An  $n$ th-order, autonomous, nonlinear system is represented by the state equation with initial condition<sup>1</sup>

$$\dot{\underline{x}} = \underline{f}(\underline{x}), \quad \underline{x}(t = 0) = \underline{x}_0. \quad (22)$$

<sup>1</sup> The derivation, presented in this appendix, is taken from [16].

The solution to this equation is written as  $\phi_t(x_0)$ , so

$$\dot{\phi}_t(x_0) = f(\phi_t(x_0)), \quad \phi_0(x_0) = x_0. \quad (23)$$

Differentiating with respect to  $x_0$  gives

$$\frac{\partial \dot{\phi}_t(x_0)}{\partial x_0} = \frac{\partial f}{\partial x} \frac{\partial \phi_t(x_0)}{\partial x_0}, \quad \frac{\partial \phi_0(x_0)}{\partial x_0} = \underline{I}. \quad (24)$$

Defining  $\Phi_t(x_0) \equiv \partial \phi_t(x_0) / \partial x_0$ , Equation (24) becomes

$$\dot{\Phi}_t(x_0) = \frac{\partial f}{\partial x} \Phi_t(x_0), \quad \Phi_0(x_0) = \underline{I}, \quad (25)$$

which is the *variational equation*. The fundamental solution matrix after a period time  $T$  is called the monodromy matrix  $\Phi_T$ .

## Appendix B: Parameter Values

$$\begin{aligned} l &= 0.32 \text{ m} & d &= 1 \text{ mm} \\ f_t &= 50 \text{ N} & G &= 79.6 \cdot 10^9 \text{ N/m}^2 \\ \rho &= 7850 \text{ kg/m}^3 & A &= \frac{1}{4} \pi d^2 \\ I_p &= \frac{\pi}{32} d^4 & m &= \frac{1}{3} \rho A l \\ k &= 4 \frac{f_t}{l} & k_t &= 4 \frac{G I_p}{l} \\ J &= \frac{1}{3} \rho I_p l & \delta &= 0.5 \text{ s/m} \\ F_s &= 1 \text{ N} & v_{dr} &= 1 \text{ m/s} \end{aligned}$$

## References

1. Aizerman, M. A. and Gantmakher, F. R., 'On the stability of periodic motions', *Journal of Applied Mathematics and Mechanics* **22** 1958, 1065–1078 [translated from Russian].
2. Andersson, I., 'Stick-slip motion in one-dimensional continuous systems and systems with several degrees-of-freedom', Ph.D. Thesis, Chalmers University of Technology, Göteborg, Sweden, 1980.
3. Armstrong-Hélouvry, B., Dupont, P., and Canudas De Wit, C., 'A survey of models, analysis tools and compensation methods for the control of machines with friction', *Automatica* **30**(7), 1994, 1083–1138.
4. Ascher, U. M., Mattheij, R. M. M., and Russell, R. D., *Numerical Solution of Boundary Value Problems for Ordinary Differential Equations*, Society for Industrial and Applied Mathematics, Philadelphia, 1995.
5. Bockman, S. F., 'Lyapunov exponents for systems described by differential equations with discontinuous right-hand sides', in *Proceedings of the American Control Conference*, Vol. 2, 1991, pp. 1673–1678.
6. Brockley, C. A. and Ko, P. L., 'Quasi-harmonic friction-induced vibration', *ASME Journal of Lubrication Technology* **92**, 1970, 550–556.
7. Galvanetto, U., Bishop, S. R., and Briseghella, L., 'Mechanical stick-slip vibrations', *International Journal of Bifurcation and Chaos* **5**(3), 1995, 637–651.

8. Haessig, Jr., D. A. and Friedland, B., 'On the modeling and simulation of friction', *ASME Journal of Dynamic Systems, Measurement and Control* **113**, 1991, 354–362.
9. Ibrahim, R. A., 'Friction-induced vibration, chatter, squeal and, chaos; Part I: Mechanics of contact and friction', *ASME Applied Mechanics Reviews* **47**(7), 1994, 209–226.
10. Ibrahim, R. A., 'Friction-induced vibration, chatter, squeal and, chaos; Part II: Dynamics and modeling', *ASME Applied Mechanics Reviews* **47**(7), 1994, 227–253.
11. Karnopp, D., 'Computer simulation of stick-slip friction in mechanical dynamic systems', *ASME Journal of Dynamic Systems, Measurement and Control* **107**, 1985, 100–103.
12. Kato, S., Sato, N., and Matsubayashi, T., 'Some considerations on characteristics of static friction of machine tool slideway', *Journal of Lubrication Technology* **94**, 1972, 234–247.
13. Kleczka, W. and Kreuzer, E., 'On approximations of non-smooth functions in bifurcation analysis', in *Nonlinearity and Chaos in Engineering Dynamics*, J. M. T. Thompson and S. R. Bishop (eds.), Wiley, Chichester, 1994, pp. 115–123.
14. Meijaard, J. P., 'Efficient numerical integration of the equations of motion of non-smooth mechanical systems', *Zeitschrift für Angewandte Mathematik und Mechanik* **77**(6), 1997, 419–427.
15. Müller, P. C., 'Calculation of Lyapunov exponents for dynamic systems with discontinuities', *Chaos, Solitons and Fractals* **5**(9), 1995, 1671–1681.
16. Parker, T. S. and Chua, L. O., *Practical Numerical Algorithms for Chaotic Systems*, Springer-Verlag, New York, 1989.
17. Pfeiffer, F., 'Dynamical systems with time-varying or unsteady structure', *Zeitschrift für Angewandte Mathematik und Mechanik* **71**(4), 1991, T6–T22.
18. Popp, K., 'Some model problems showing stick-slip motion and chaos', in *ASME WAM, Proceedings Symposium on Friction Induced Vibration, Chatter, Squeal, and Chaos*, Vol. 49, R. A. Ibrahim and A. Soom (eds.), ASME, New York, 1992, pp. 1–12.
19. Popp, K., Hinrichs, N., and Oestreich, M., 'Dynamical behaviour of a friction oscillator with simultaneous self and external excitation', *Sādhāna: Academy Proceedings in Engineering Sciences*, Part 2–4, **20**, 1995, 627–654.
20. Sepehri, N., Sassani, F., Lawrence, P. D., and Ghasemipoor, A., 'Simulation and experimental studies of gear backlash and stick-slip friction in hydraulic excavator swing motion', *ASME Journal of Dynamic Systems, Measurement and Control* **118**, 1996, 463–467.
21. Stelzer, P., 'Nonlinear vibrations of structures induced by dry friction', *Nonlinear Dynamics* **3**, 1992, 329–345.
22. Van de Vorst, E. L. B., 'Long term dynamics and stabilization of nonlinear mechanical systems', Ph.D. Thesis, Eindhoven University of Technology, Eindhoven, The Netherlands, 1996.
23. Van de Vrande, B. L., Van Campen, D.H., and De Kraker, A., 'Some aspects of the analysis of stick-slip vibrations with an application to drillstrings', in *Proceedings of ASME Design Engineering Technical Conference*, 16th Biennial Conference on Mechanical Vibration and Noise, DETC/VIB-4109, published on CD-ROM, 8 pp., Sacramento, September 14–17, 1997.